

# Voltage-controlled coded qubit based on electron spin

Pawel Hawrylak and Marek Korkusinski

Quantum Theory Group, Institute for Microstructural Sciences,  
National Research Council of Canada,  
Ottawa, Ontario, Canada K1A 0R6

## Abstract

We design and analyze a solid state qubit based on electron spin and controlled by electrical means. The coded qubit is composed of a three-electron complex in three tunable gated quantum dots. The two logical states  $|0\rangle_L$  and  $|1\rangle_L$  of a qubit reside in a degenerate subspace of total spin  $S = 1/2$  states. We demonstrate how applying voltages to specific gates changes the one-electron properties of the structure, and show how electron-electron interaction translates these changes into the manipulation of the two lowest energy states of the three-electron complex.

PACS numbers: 73.21.La (Quantum dots), 03.67.Lx (Quantum computation) 85.75.Hh (Spin polarized field effect transistors)

## I. INTRODUCTION

Considerable experimental and theoretical effort is currently being applied towards the realisation of scalable quantum bits and gates.<sup>1,2,3,4,5</sup> Electron spin-based qubits are considered to be viable candidates due to demonstrated long coherence times.<sup>6,7,8</sup> For single quantum dots<sup>8,9,10</sup> it is now possible to isolate, control, and exploit the spin properties of electron at the single-spin level.<sup>10,11</sup> Simultaneously, progress has been made in coupled quantum dot systems, where control of electron numbers in individual dots and coupling between the dots necessary to realise the building blocks for quantum information processing<sup>11,12,13,14,15,16</sup> has been demonstrated. Despite this progress many obstacles need to be overcome before elementary quantum operations on electron spin-based qubits<sup>17,18,19,20</sup> can be demonstrated. One of the fundamental challenges is the task of isolating a single-electron spin and contacting it to perform single-qubit operations. This challenge stems from the need to produce a localised and switchable magnetic field required for spin manipulation. A number of solutions have been proposed<sup>21,22,23,24</sup> to replace the local magnetic field by locally engineered coupling (g-factor) to the constant magnetic field. The g-factor engineering has to be combined with equally challenging spatial manipulation of electron position using surface gates. To date, even single-qubit operation of qubits based on electron spin still awaits demonstration. An alternative solution to the problem of qubit operations on a single spin was proposed by DiVincenzo, Lidar and collaborators,<sup>25,26,27</sup> who suggested quantum computation with exchange interaction. The basic idea is to replace the two-level system based on the single-electron spin with selected levels of a composite object consisting of several spins. The manipulation of selected quantum levels proceeds not through operations on single spins but through manipulation of the coupling  $J$  between neighbouring spins due to exchange interaction. For example, two qubit states  $|j_i\rangle$  and  $|j_l\rangle$  for a single total spin  $S = 1=2$  can be identified with two opposite spin directions ( $S_z$ ) up and down:  $|j_i\rangle = |j\#i\rangle$  and  $|j_l\rangle = |j"i\rangle$ . By contrast, in a coded qubit consisting of three localised electron spins (a, b, c) we start by selecting a total spin  $S_z$  of the three spins, e.g.,  $|j\#i\rangle$ . A state with this direction can be realised by three different states:  $|j\#a;\#b;"c\rangle$ ,  $|j\#a;"b;\#c\rangle$ , and  $|j"a;\#b;\#c\rangle$ , which differ by the position of the spin pointing up. We can group these three states into a single state with total spin  $S = 3=2$  and two orthogonal states with total spin  $S = 1=2$ . Examples of the two orthogonal spin states forming the two

logical qubit states  $|0\rangle_L$  and  $|1\rangle_L$  are  $|0\rangle_L = \frac{1}{\sqrt{2}}(|j \# a; \# b; \# c\rangle + |j \# a; \# b; \# c\rangle)$  and  $|1\rangle_L = \frac{1}{\sqrt{6}}(|j \# a; \# b; \# c\rangle + |j \# a; \# b; \# c\rangle - 2|j \# a; \# b; \# c\rangle)$ .

The properties of a three-electron complex in a single quantum dot, including the two logical spin states discussed above, have been analyzed previously.<sup>28,29</sup> The three-electron states are a product of the orbital and spin part. The spin part has been discussed in terms of the logical qubit states. But it is precisely the orbital part, and specifically the one-electron wave function, that can be manipulated using voltages, and hence it plays a crucial role in a coded qubit. In what follows we employ the methodology which allowed for a quantitative understanding of a single dot with controlled number of electrons<sup>30</sup> to study the energy levels and spin and orbital wave functions of a realistic coded qubit. We show that there exist two low-energy states which map very well onto the two logical qubit states, and that they can be manipulated by applied voltages. Section 2 describes the model of a qubit, Section 3 describes its one electron properties, Section 4 contains results of numerical simulation of a three electron complex, Section 5 describes the Hubbard model of the qubit and elucidates the physics, and conclusions are contained in Section 6.

## II. THE MODEL

The proposed device is shown in Fig. 1a. It consists of a metallic gate defining three coupled lateral quantum dots. The dots are defined by locally depleting the two-dimensional electron gas (2DEG) at a distance  $D$  below the surface. Application of a negative voltage creates a broad region depleted of electrons, with three identical minima. An additional gate (the control gate  $V_x$ ), shown in red, is positioned in-between the two adjacent dots 1 and 2. The gate  $V_x$  lowers or increases the tunnelling barrier between the two dots. As we will show, the effect of the gate is identical to the effect of the  $\sigma_x$  operation acting on logical qubit states. The  $\sigma_x$  acting on logical qubit  $|0\rangle_L$  transforms it into qubit  $|1\rangle_L$  and vice versa. The manifestation of the  $\sigma_x$  operation is the energy splitting  $\Delta_x$  of the two degenerate logical qubit states. In order to have complete logical qubit rotation we need a second gate. This gate, labelled  $V_z$ , plays the role of  $\sigma_z$  spin operation, and in our model it tunes the potential minimum of the third dot. Finally, we need to precisely control the number of electrons  $N = 3$  in our device. This can be accomplished by following the detailed design which allowed to control the number of electrons in single and coupled quantum dots.<sup>10,11</sup>

The electronic properties are determined by the confining potential produced by the gates and by the positive potential of donors. Once the number of electrons in the device is fixed, the donor potential plays no role and is neglected here. The operation of gates translates into the changes of a potential seen by each of the three electrons in a coded qubit. The electrostatic potential  $V_E(\mathbf{r})$  in the electronic plane due to the gates on the surface is given by an integral over the potential  $V_G(\mathbf{r}^0)$  applied to the gates as<sup>30,31</sup>

$$V_E(\mathbf{r}) = \frac{1}{2} \int \frac{V_G(\mathbf{r}^0)}{(D^2 + (\mathbf{r} - \mathbf{r}^0)^2)^{3/2}} d\mathbf{r}^0; \quad (1)$$

where  $D$  is the distance between the surface and the 2D E $\bar{G}$  layer, and  $V_G(\mathbf{r})$  is the electrical potential on the surface, corresponding to the appropriate voltage on the gates, and equal to zero in the openings (the holes). In our calculation, we express all energies and distances in the units of effective Rydberg,  $R = m^* e^4 / (2 \hbar^2 \epsilon^2)$ , and effective Bohr radius,  $a_B = \hbar^2 / m^* e^2$ , respectively. Here,  $e$  and  $m^*$  are the electronic charge and effective mass, respectively,  $\epsilon$  is the dielectric constant of the semiconductor, and  $\hbar$  is the Dirac's constant. For GaAs these units are  $1R = 5.93 \text{ meV}$ , and  $1a_B = 97.9 \text{ \AA} = 10 \text{ nm}$ . The candidate for a coded qubit investigated here has the length of the side of the rectangular gate of  $22.4 a_B$  (for better visibility of the potential minima, in Fig. 1 we only show a central part of the gate, with side length of  $14 a_B$ ). The diameter of the opening (the hole) in the gate is taken to be  $4.2 a_B$ , the distance between the centers of each pair of holes is  $4.85 a_B$ , and the distance between the gate and the 2D E $\bar{G}$  layers is  $14 a_B$ . The voltage applied to the main gate corresponds to the electronic potential energy  $eV = 10 R$  in the plane of the gates. As shown in Fig. 1, the pattern of the holes in the surface gate translates into three potential minima on the electronic plane. As illustrated in Fig. 1a, if the voltage of the control gate  $V_x$  is set to zero, the three potential minima are identical. But if we apply voltage  $eV = -10 R$ , i.e., opposite to that of the main gate, the barrier between two of the dots is lowered and the dots 1 and 2 are strongly coupled. Note that the two other tunnelling barriers are weakly affected by the control gate. The voltage applied to the gates couples to the charge of the electron and determines the potential  $V_E$  acting on each individual electron.

### III. THE ONE-ELECTRON PROPERTIES

The potential determines the single-electron energies  $E_n$  and wave functions  $\psi_n(x; y)$ . The external voltages applied to control gates affect directly only single-electron properties, and through the modification of single-electron energies and wave functions – the states of the three-electron complex. To calculate the single-electron spectrum we discretize the area under the gates, and define the single-electron states  $\psi_n(x; y)$  on a lattice  $(x_i; y_j)$  with spacing  $h$ . Electrons move on a lattice, and their spectrum is described by the tight-binding Hamiltonian:

$$(\epsilon_{i;j} + V_E(i; j)) \psi_n(i; j) + \sum_{k;l} t_{i;j;k;l} \psi_n(k; l) = E_n \psi_n(i; j); \quad (2)$$

where the site energy and hopping matrix elements are given by  $\epsilon_{i;j} = 4h^{-2}$  and  $t_{i;j;k;l} = h^{-2} \delta_{k;i-1; l;j}$ , respectively. As a result we obtain a large, but sparse Hamiltonian matrix, which is diagonalized using the conjugate gradient method. In Fig. 2a we show the calculated energies  $E_n$  corresponding to nine lowest single-particle states as a function of the potential  $V_x$  of the control gate. At zero bias the spectrum consists of three energy levels, the ground state and two degenerate excited states, separated by a gap from the rest of the spectrum. The corresponding three lowest single-particle wave functions at zero bias are shown in Fig. 2b. The states and the energy spectrum can be understood by considering a linear combination of wave functions  $f_m(x; y)$  localized on  $m$ -th dot. The corresponding ground state can be written as  $|\psi_0\rangle = \frac{1}{\sqrt{3}}(f_1(x; y) + f_2(x; y) + f_3(x; y))$ , and the two degenerate excited states as  $|\psi_1\rangle = \frac{1}{\sqrt{6}}(f_1(x; y) + f_2(x; y) - 2f_3(x; y))$  and  $|\psi_2\rangle = \frac{1}{\sqrt{2}}(f_1(x; y) - f_2(x; y))$ . In all of these states the electron is delocalised and shared between all dots. For negative gate voltages, i.e., when the barrier between the two dots is lowered, the two excited states mix and energy levels split. When the voltage is zero, the three dots are identical, and the two excited states are degenerate. As the barrier between the two dots is increased even further (positive gate voltages), the energies of degenerate states are split again. In this case, however, the splitting is not large. We attribute it to the fact that, in this regime, all interdot barriers are already high and the three dots are almost isolated. Therefore, a further increase of the control gate voltage increases the total energy of the system, but does not lead to a significant symmetry breaking.

#### IV . THREE ELECTRONS - NUMERICAL APPROACH

Now that we understand the effect of gate voltages on a single electron, we proceed to consider three electrons localized in our three-dot potential.

We describe simultaneously the spin and orbital three-electron states in the language of second quantization as  $|j_i; j^0; k^0\rangle = c_1^\dagger c_j^\dagger c_k^\dagger |0\rangle$ . The operator  $c_i^\dagger$  ( $c_i$ ) creates (annihilates) an electron with spin  $\uparrow$  on the single-particle state  $|i\rangle$  calculated from Eq. 2. The electron-electron interactions mix different three-electron configurations for a given set of applied voltages. The mixing is governed by the matrix elements of the Hamiltonian, which takes the form :

$$H = \sum_i E_i c_1^\dagger c_i + \frac{1}{2} \sum_{ijkl} h_{ijkl} c_1^\dagger c_j^\dagger c_k^\dagger c_l; \quad (3)$$

where the energies  $E_i(V_x; V_z)$  and matrix elements  $h_{ijkl}(V_x; V_z)$  of the Coulomb potential are implicit functions of the applied voltages  $V_x, V_z$ . These matrix elements are independent of spin. They are calculated in real space as

$$h_{ijkl} = 2h^3 \sum_{sp; uv} \frac{\psi_i(s; p) \psi_j(u; v) \psi_k(u; v) \psi_l(s; p)}{[(s-u)^2 + (p-v)^2 + d^2]^{1/2}}; \quad (4)$$

with parameter  $d$  accounting for the finite thickness of the electron layer (in the following example we take  $d = 0.2 a_B$ ). To capture spin effects we generate all possible configurations of three electrons on  $N_S$  single-particle states and classify them by total spin.<sup>32</sup> This allows us to construct the Hamiltonian matrix separately in the spin  $S=2$  and spin  $S=1$  basis and diagonalize these matrices numerically. Figure 3 shows the low-energy segment of the three-electron energy spectrum as a function of the voltage on the control gate  $V_x$  (the energies are measured from the ground-state energy). The low-energy spectrum consists of two low-energy states corresponding to the two states of the  $S = 1$  Hilbert space (black lines), while the energy of the higher state corresponds to the high-spin  $S = 3/2$  state (red line). The fact that the two  $S = 1$  logical qubit states are the lowest energy states is important as it facilitates the initialization of a qubit. It is also a rather counterintuitive result as one might expect exchange to favor spin polarized state. The central result of this paper rests on the identification of the two lowest energy  $S = 1$  states of a three electron complex as the two logical states of the coded qubit. The two logical states can be manipulated by applying gate voltage  $V_x$ , which shifts the energy of the two levels, as seen in Figure 3. The

voltage  $V_x$  acts analogously to the  $\sigma_x$  operation, while the  $\sigma_z$  operation can be implemented by applying voltage  $V_z$ .

The remaining concern is that the two logical qubit states be well isolated from other states with the same total spin. The inset in Fig. 3 shows the energy spectrum over larger energy scale, with a significant gap in the energy spectrum between the two logical qubit states and the remaining  $S = 1=2$  states.

## V. THREE ELECTRONS-HUBBARD MODEL

The principle of operation of this device, and the analogy to the two-spin logical qubit states can be understood by considering a simplifying model of the coded qubit. The model starts with the single-particle spectrum of Fig. 2, described in terms of linear combinations of orbitals localised on each dot  $\{1, 2, 3\}$ . With the energies of one localised orbital per dot denoted by  $E_n$  ( $n=1, 2, 3$ ), hopping matrix element  $t_{n,m}$  from dot  $n$  to dot  $m$ , and on-site Coulomb repulsion  $U$ , we can analyze the coded qubit in the framework of a three-site Hubbard model. We start with the completely polarized system, i.e., one with total spin  $S = 3=2$ . We can distribute our electrons on the three sites in only one way: one electron on each site, which gives a spin-polarized state  $|\alpha_{3=2}\rangle = c_{3\#}^\dagger c_{2\#}^\dagger c_{1\#}^\dagger |0\rangle$ . As the basis of our Hilbert space consists of one configuration only,  $|\alpha_{3=2}\rangle$  is the eigenstate of our system, and its energy  $E_{3=2} = E_1 + E_2 + E_3$ . Let us now flip the spin of one of the electrons. This electron can be placed on any orbital, and as a result we can generate nine different configurations. Three of those configurations involve single occupancy of the orbitals. They can be written as  $|\beta\rangle = c_{3\#}^\dagger c_{2\#}^\dagger c_{1\#} |0\rangle$ ,  $|\gamma\rangle = c_{1\#}^\dagger c_{3\#}^\dagger c_{2\#} |0\rangle$ , and  $|\delta\rangle = c_{2\#}^\dagger c_{1\#}^\dagger c_{3\#} |0\rangle$ . Out of these three configurations we construct the three eigenstates of the total spin operator. One of those eigenstates is  $|\beta_{3=2}\rangle = \frac{1}{\sqrt{3}} (|\beta\rangle + |\gamma\rangle + |\delta\rangle)$ , and it corresponds to the total spin  $S = 3=2$ . The two other eigenstates,  $|\beta_{1=2}\rangle = \frac{1}{\sqrt{2}} (|\beta\rangle - |\gamma\rangle)$  and  $|\gamma_{1=2}\rangle = \frac{1}{\sqrt{6}} (|\beta\rangle + |\gamma\rangle - 2|\delta\rangle)$ , correspond to the total spin  $S = 1=2$ . The remaining six configurations involve doubly-occupied orbitals. They are  $|\beta_{1=2}\rangle = c_{2\#}^\dagger c_{1\#}^\dagger c_{3\#} |0\rangle$ ,  $|\gamma_{1=2}\rangle = c_{3\#}^\dagger c_{1\#}^\dagger c_{2\#} |0\rangle$ ,  $|\delta_{1=2}\rangle = c_{2\#}^\dagger c_{1\#}^\dagger c_{2\#} |0\rangle$ ,  $|\beta_{1=2}\rangle = c_{3\#}^\dagger c_{2\#}^\dagger c_{1\#} |0\rangle$ ,  $|\gamma_{1=2}\rangle = c_{3\#}^\dagger c_{1\#}^\dagger c_{3\#} |0\rangle$ , and  $|\delta_{1=2}\rangle = c_{3\#}^\dagger c_{2\#}^\dagger c_{3\#} |0\rangle$ . All these configurations are eigenstates of the total spin with  $S = 1=2$ . Thus, among our nine spin-unpolarized states we have one high-spin, and eight low-spin states. In this basis the Hamiltonian matrix is block-diagonal, with the high-spin state completely decoupled. The energy corresponding

to this state is equal to that of the fully polarized system discussed above, and is  $E_{3=2}$ . We construct the Hamiltonian matrix in the basis of the nine  $S = 1/2$ -spin configurations by dividing them into three groups, each containing one of the singly-occupied configurations  $\mathcal{A}i = c_{3\#}^\dagger c_{2\#}^\dagger c_{1\#}^\dagger |i\rangle$ ,  $\mathcal{B}i = c_{1\#}^\dagger c_{3\#}^\dagger c_{2\#}^\dagger |i\rangle$ , and  $\mathcal{C}i = c_{2\#}^\dagger c_{1\#}^\dagger c_{3\#}^\dagger |i\rangle$ , which are needed to construct a coded qubit. By labelling each group with an index of spin-up electron, the Hamiltonian takes the form of a  $3 \times 3$  matrix:

$$\hat{H}_{1=2} = \begin{matrix} & \begin{matrix} 2 & & 3 \end{matrix} \\ \begin{matrix} \hat{H}_1 & \hat{T}_{12} & \hat{T}_{13} \\ \hat{T}_{12} & \hat{H}_2 & \hat{T}_{23} \\ \hat{T}_{13} & \hat{T}_{23} & \hat{H}_3 \end{matrix} & \begin{matrix} 7 \\ 7 \\ 5 \end{matrix} \end{matrix} : \quad (5)$$

The diagonal matrix, e.g.,

$$\hat{H}_1 = \begin{matrix} & \begin{matrix} 2 & & 3 \end{matrix} \\ \begin{matrix} 6 \\ 6 \\ 6 \\ 4 \end{matrix} & \begin{matrix} 2E_1 + E_2 + U_1 & & \\ & t_{23} & & \\ & & 2E_1 + E_3 + U_1 & \\ & & & E_1 + E_2 + E_3 \end{matrix} & \begin{matrix} 7 \\ 7 \\ 7 \\ 5 \end{matrix} \end{matrix}$$

describes the interaction of three configurations which contain spin up electron on site "1", i.e., two doubly-occupied configurations  $\mathcal{B}_{2=2}i = c_{2\#}^\dagger c_{1\#}^\dagger c_{1\#}^\dagger |i\rangle$  and  $\mathcal{C}_{1=2}i = c_{3\#}^\dagger c_{1\#}^\dagger c_{1\#}^\dagger |i\rangle$ , and a singly-occupied configuration  $\mathcal{A}i = c_{3\#}^\dagger c_{2\#}^\dagger c_{1\#}^\dagger |i\rangle$  (in this order). The configurations with double occupancy acquire the diagonal interaction term  $U$ . The three configurations involve a pair of spin-polarized electrons (spin triplet) moving on a triangular plaquette in the presence of a "spectator" spin-up electron. Because of the triplet character of the two electrons, the phase of the hopping matrix element  $t_{13}$  from site "1" to site "3" is different from the phase of the hopping matrix element  $t_{23}$  from site "2" to site "3". The negative phase in  $t_{13}$  distinguishes singlet and triplet electron pairs, lowers the energy of the spin-polarized pair in the absence of interactions, and is a manifestation of the "orbital Hund's rule".<sup>33</sup> The orbital Hund's rules are responsible for dressing up of the desired singly occupied configuration by the doubly occupied configuration, and by the interaction of the coded qubit states. It is clear that the simple model discussed here contains a rich and nontrivial behaviour. The remaining matrices corresponding to spin-up electrons localized on sites "2" and "3" can be constructed in a similar fashion:

$$\hat{H}_2 = \begin{matrix} & \begin{matrix} 2 & & 3 \end{matrix} \\ \begin{matrix} 6 \\ 6 \\ 6 \\ 4 \end{matrix} & \begin{matrix} E_1 + 2E_2 + U_2 & & \\ & t_{23} & & \\ & & E_1 + E_2 + E_3 & \\ & & & 2E_2 + E_3 + U_2 \end{matrix} & \begin{matrix} 7 \\ 7 \\ 7 \\ 5 \end{matrix} \end{matrix} ;$$



and design of complex qubit circuits remains to be investigated, it appears that coded qubits based on electron spin are promising devices for quantum information processing.

Acknowledgement. M.K. acknowledges financial support from the Natural Sciences and Engineering Research Council of Canada and P.H. acknowledges the support from the Canadian Institute for Advanced Research. The authors thank A. Sachrajda, G. Austing and G. Sawatzky for discussions.

- 
- <sup>1</sup> Feynman, R.P., *Foundations of Physics* 16, 507 (1986).
  - <sup>2</sup> Bennett, C.H. and DiVincenzo, D.P., *Nature* 404, 247 (2000).
  - <sup>3</sup> Nielsen, M.A., Knill, E., and Laflamme, R., *Nature* 396, 52 (1998).
  - <sup>4</sup> Vandersypen, L.M., et al., *Nature* 414, 883 (2001).
  - <sup>5</sup> Bayer, M., et al., *Science* 291, 451 (2001).
  - <sup>6</sup> Awschalom, D.D. and Kikkawa, J.M., *Phys. Today* 6, 33 (1999).
  - <sup>7</sup> Fujisawa, T., et al., *Nature* 419, 278 (2002).
  - <sup>8</sup> Hanson, R., et al., *Phys. Rev. Lett.* 91, 196802 (2003).
  - <sup>9</sup> Tarucha, S., et al., *Phys. Rev. Lett.* 77, 3613 (1996).
  - <sup>10</sup> Ciorga, M., et al., *Phys. Rev. B* 61, R16315 (2000).
  - <sup>11</sup> Pioro-Ladriere, M., et al., *Phys. Rev. Lett.* 91, 026803 (2003).
  - <sup>12</sup> Livemore, C., et al., *Science* 274, 1332 (1996).
  - <sup>13</sup> Oosterkamp, T.H., et al., *Nature* 395, 873 (1998).
  - <sup>14</sup> Duncan, D.S., et al., *Phys. Rev. B* 63, 045311 (2001).
  - <sup>15</sup> Holleitner, A.W., et al., *Science* 297, 70 (2001).
  - <sup>16</sup> Craig, N.J., et al., *Science* 304, 565 (2004).
  - <sup>17</sup> Brum, J.A. and Hawrylak, P., *Superlatt. Microstruct.* 22, 431 (1997).
  - <sup>18</sup> Loss, D. and DiVincenzo, D.P., *Phys. Rev. A* 57, 120 (1998).
  - <sup>19</sup> Ciorga, M., et al., *Physica E* 11, 35 (2001).
  - <sup>20</sup> Kane, B.E., *Nature* 393, 133 (1998).
  - <sup>21</sup> Kato, Y., et al., *Nature* 427, 50 (2004).
  - <sup>22</sup> Rashba, E.I. and Efros, A.L., *Phys. Rev. Lett.* 91, 126405 (2003).
  - <sup>23</sup> M.Xiao, I.Martin, E.Yablonovitch, and H.W. Jiang, *Nature* 430, 435 (2004).

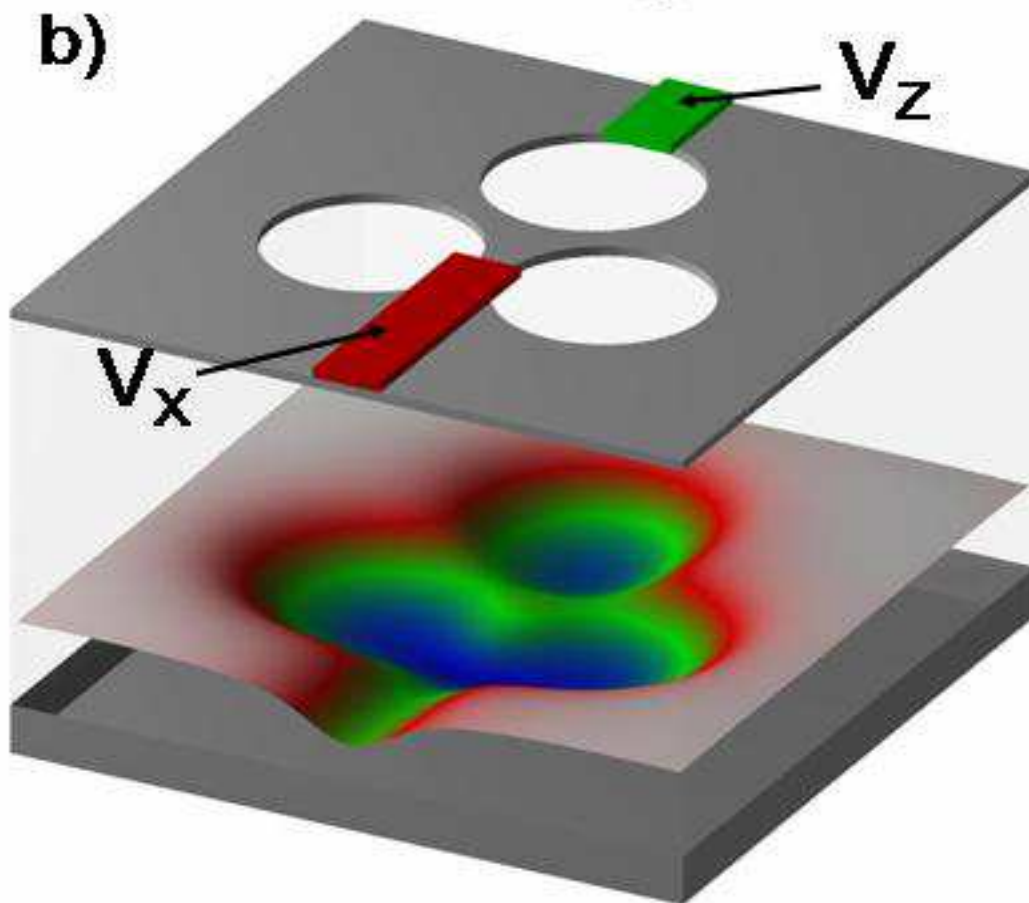
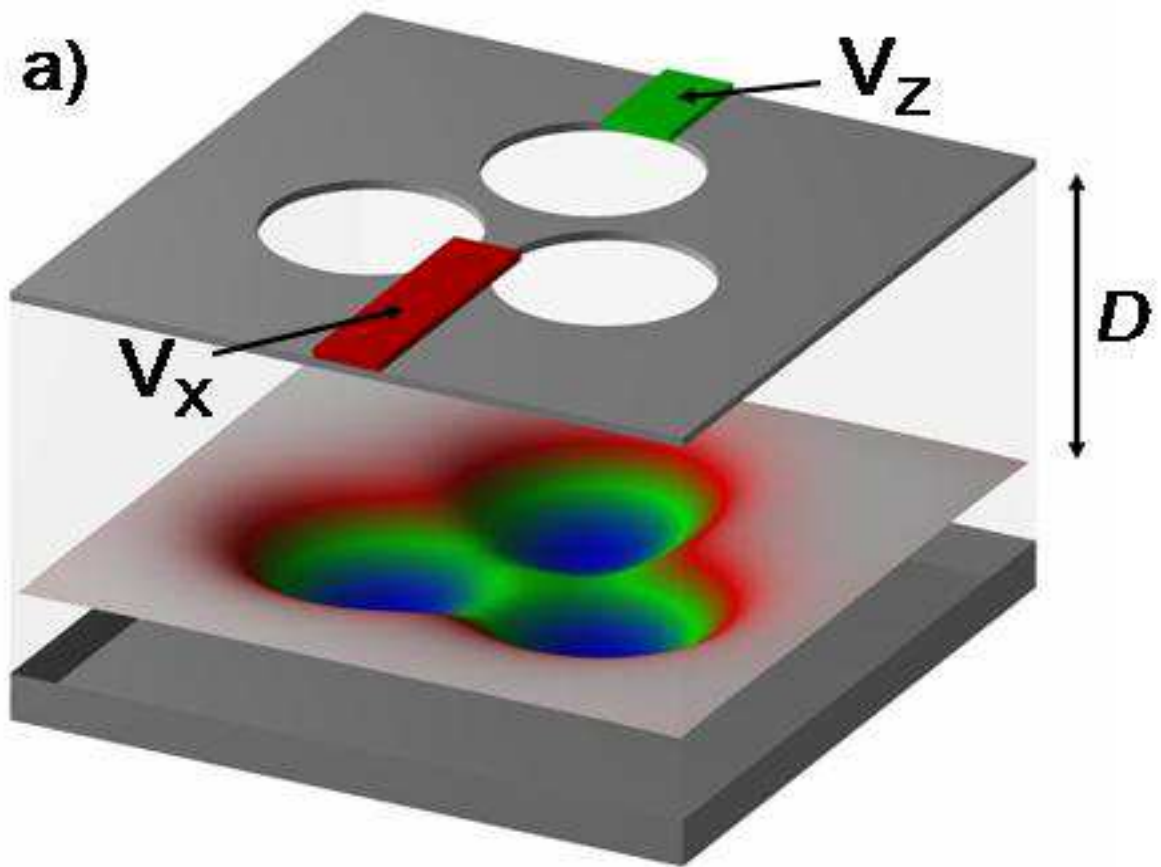
- <sup>24</sup> Elzerman, J. M. ., Hanson, R. ., Willem s van Beveren, L. H. ., Witkamp, B. ., Vandersypen, L. M. .  
K. ., and Kouwenhoven, L. P. ., Nature 430, 431 (2004).
- <sup>25</sup> Di Vincenzo, D. P., et al., Nature 408, 339 (2000).
- <sup>26</sup> Bacon, D. ., et al., Phys. Rev. Lett. 85, 1758 (2000).
- <sup>27</sup> Mizel, A. . and Lidar, D. A. ., Phys. Rev. Lett. 92, 077903 (2004).
- <sup>28</sup> Hawrylak, P. ., Phys. Rev. Lett. 71, 3347 (1993).
- <sup>29</sup> Ashoori, R. C. ., Nature 379, 413 (1996).
- <sup>30</sup> Kyriakidis, J. et al., Phys. Rev. B 66, 35320 (2002).
- <sup>31</sup> Davies, J. H. ., Larkin, I. A. ., and Sukhorukov, E. V. ., J. Appl. Phys. 77, 4504 (1995).
- <sup>32</sup> Wensauer, A. ., Korkusinski, M. ., and Hawrylak, P. ., Solid State Commun. 130, 115 (2004).
- <sup>33</sup> Emov, I. S. ., Yunoki, S. ., and Sawatzky, G. ., Phys. Rev. Lett. 85, 216403 (2002).

FIG . 1: Cross-sectional view of the coded qubit realized on three coupled gated lateral quantum dots. The grey rectangular gate contains three circular openings, which translate into minima of the electrostatic potential at the level of the two-dimensional electron gas. The green gate can be used to shift the potential minimum of the dot underneath with respect to the two other dots. The red gate is used to tune the tunnelling barrier between two of the dots. If this gate is not polarized (a), the three dots are identical; if its potential is equal in value and opposite in sign to that of the main gate (b), the tunnelling barrier between the two dots below is lowered.

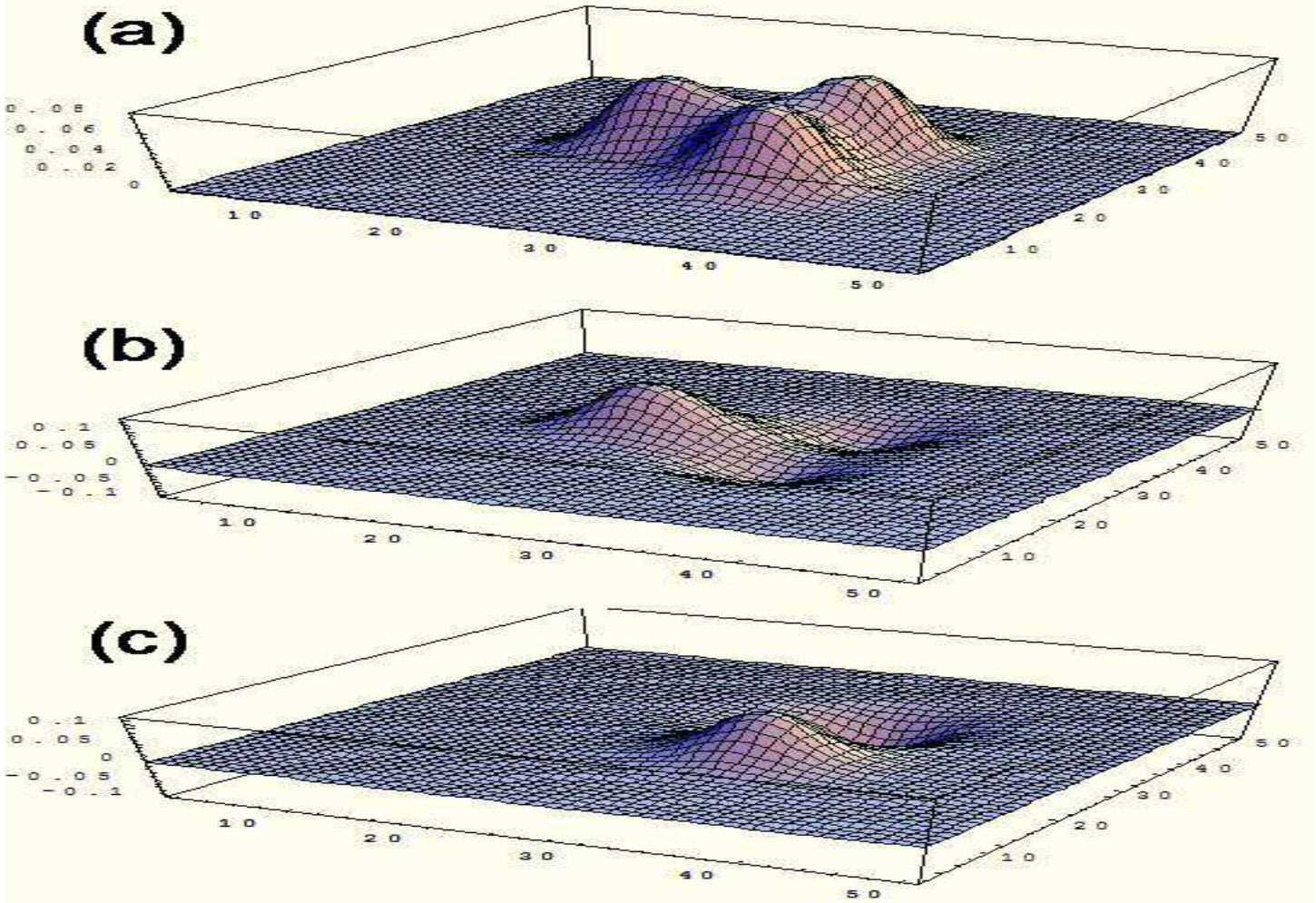
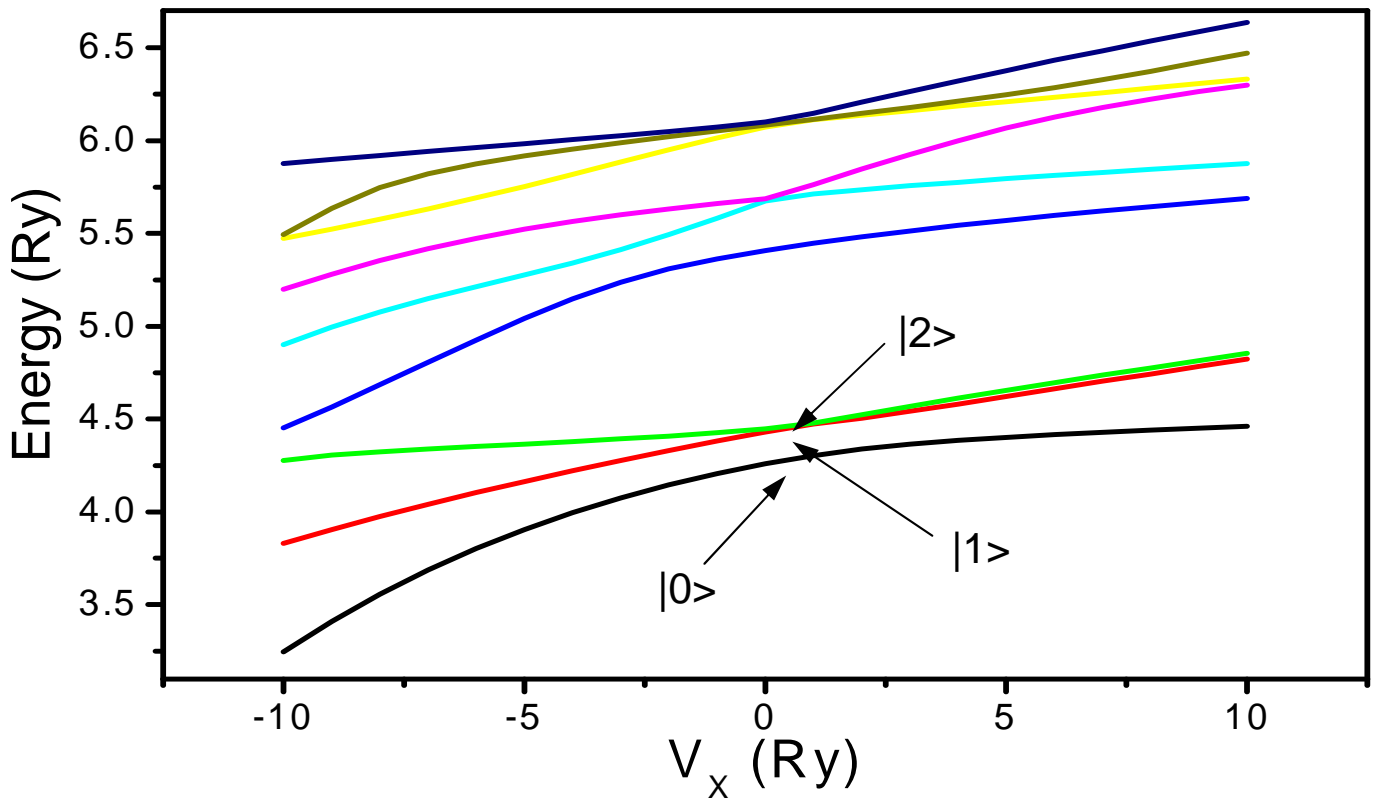
FIG . 2: (a). Energies of nine lowest single-electron levels of the three-dot system as a function of voltage applied to gate  $V_x$ . (b) Wave functions corresponding to the three lowest single-electron energy levels of the three-dot system.

FIG . 3: Energies of the three lowest states of the three-electron coded qubit as a function of the voltage applied to the control gate  $V_x$  measured from the ground state. Black lines show energies of total-spin-1=2 states identified as logical qubit states, the red line shows the energy of the spin-3=2 state. Inset shows the gap between the two logical qubit states and the rest of the spectrum as a function of the gate voltage.

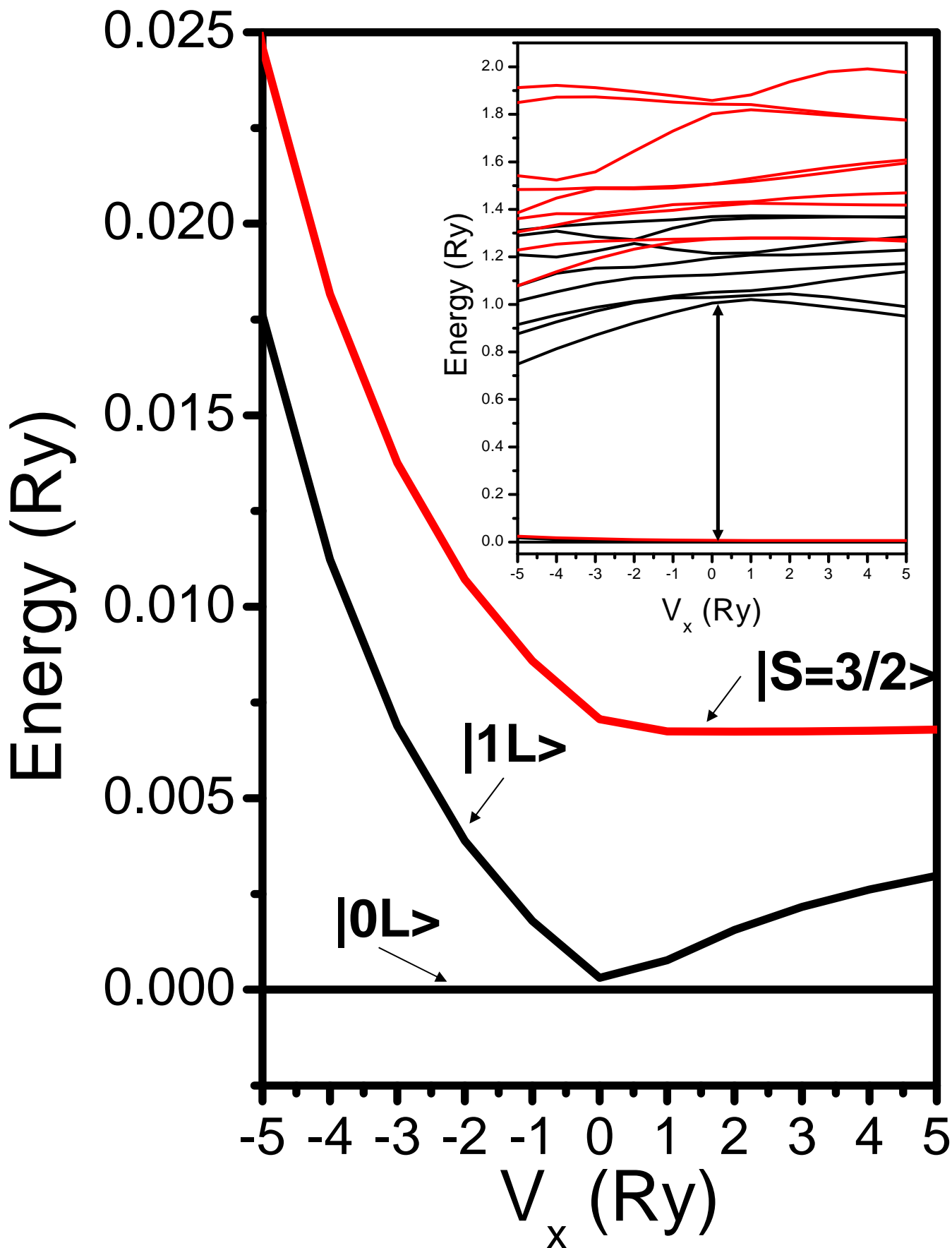
FIG. 4: Energies of three electrons localized on three Hubbard sites as a function of the tunnelling amplitude  $t_{31}$  measured from the ground state. Onsite interaction energy  $u = 3$  and  $t_{12} = t_{23} = 1$ . Black (red) lines show energies corresponding to low- (high-) spin states.



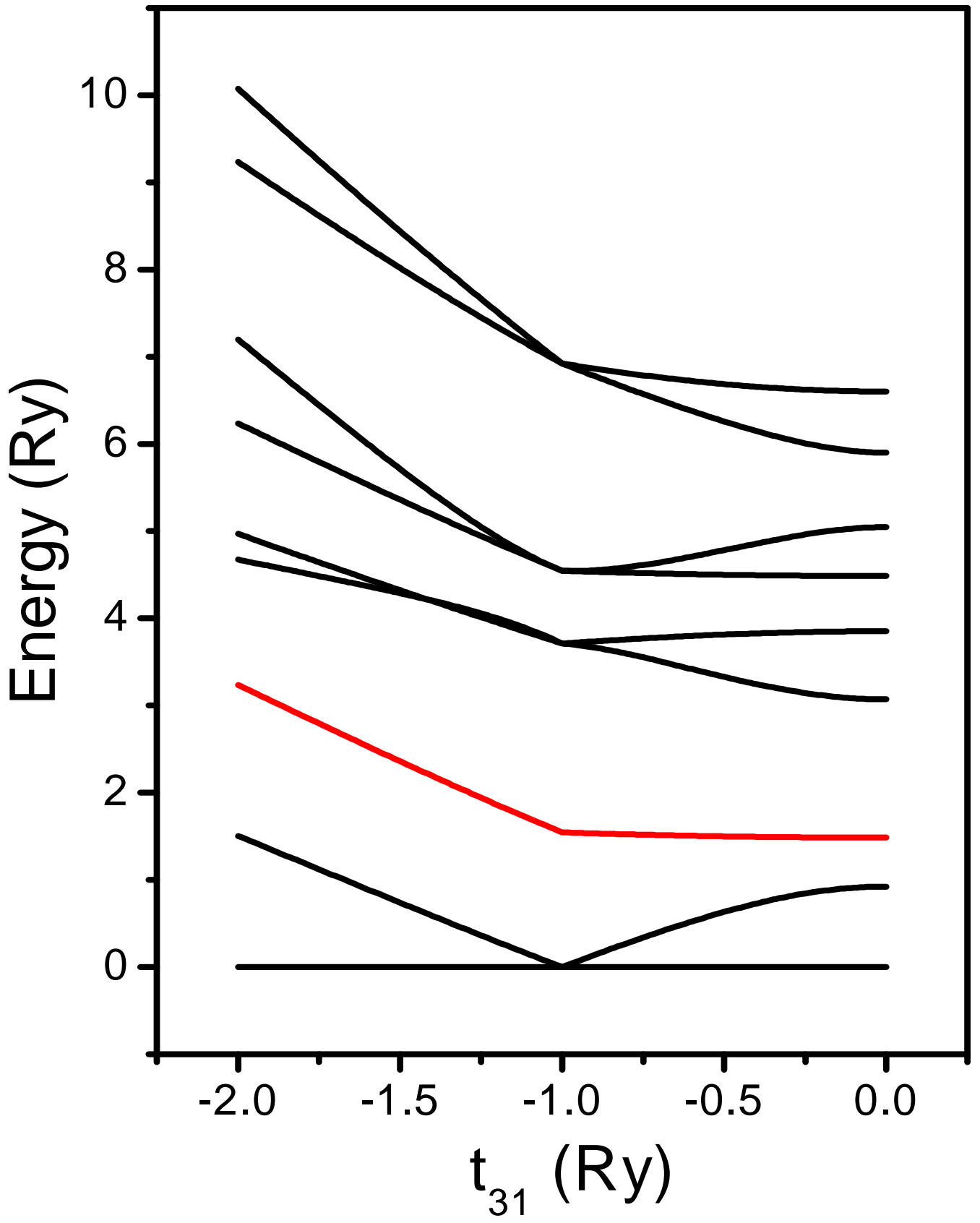
Hawrylak Figure 1



Hawrylak Figure 2



Hawrylak Figure 3



Hawrylak Figure 4